

tex, and (c) the hadron energy E_H . We have included in Fig. 4 results for SC4 alone (μ_1'), as well as for μ_1 and μ_2 . The best solid angle is achieved with μ_1 , but for μ_1' the measured values of ϵ_p are smaller than for μ_1 [Fig. 3(b)], and for μ_2 , $\epsilon_p=0$. Furthermore, the dependence on z , (x, y) , and E_H of the ϵ_μ for μ_1 , μ_1' , and μ_2 is significantly different, which serves to test the internal consistency of the data.¹¹ Apart from statistical fluctuations, Fig. 4 indicates that the same value of R is obtained from each of the muon identifiers over the entire range of each of the variables plotted and provides evidence for stability of the results. These results integrated over z , transverse position, and E_H yield

$$R = 0.20 \pm 0.05,$$

where the error includes an estimate of 0.03 for possible systematic effects, which follows from an exhaustive study of the sensitivity of R to changes in the measured variables.

The value of R measured for the combined neutrino-antineutrino beam used in this experiment is related to the values of R^ν and $R^{\bar{\nu}}$, for pure neutrinos and antineutrinos, respectively, by

$$R = aR^\nu + (1-a)R^{\bar{\nu}},$$

where $a = 0.63 \pm 0.11$ is the corrected observed ratio of the negative muon event rate to the total muon event rate. The allowed values of R^ν and $R^{\bar{\nu}}$ are presented in Fig. 4(d) which also shows the recent results for R^ν and $R^{\bar{\nu}}$ from Gargamelle.²

It is a pleasure to acknowledge the aid and encouragement of the National Accelerator Labora-

tory staff and the efforts of Robert Beck and Hans Weeden.

*Work supported in part by the U. S. Atomic Energy Commission under Contract No. AT(11-1)-881-401.

†On leave of absence from Laboratoire de L'Accélérateur Lineaire, Orsay, France.

‡Now at Stanford Linear Accelerator Center, Stanford, Calif. 94305.

§Alfred P. Sloan Foundation Fellow, now at the University of Chicago, Chicago, Ill. 60637

¹A. Benvenuti *et al.*, Phys. Rev. Lett. **32**, 1025 (1974).

²F. J. Hasert *et al.*, Phys. Lett. **46B**, 138 (1973), and CERN Report No. TC-L/Int. 74-1 (to be published).

³The horn was constructed under the supervision of F. Nezrick.

⁴A. Benvenuti *et al.*, Phys. Rev. Lett. **30**, 1084 (1973), and **32**, 125 (1974).

⁵The triggering circuitry was determined from the data to be fully efficient for hadron energy $E_H > 4$ GeV.

⁶For \overline{AEB} triggers the ratio of verticized events to all events is 0.22 for $E_H < 12$ GeV and 0.57 for $E_H > 12$ GeV, for \overline{AEB} events the corresponding ratios are 0.57 and 0.74.

⁷As Fig. 3(d) shows, the data do not indicate any excess of muonless events near the edges (142 cm) of the detector.

⁸R. W. Ellsworth *et al.*, Phys. Rev. **165**, 1449 (1968).

⁹The angle of the muon is determined from the angle of the 10-cm-long track segment in SC4 and from the line joining the track centroid to the shower vertex.

¹⁰The detection efficiency ϵ_μ includes a small correction ($\sim 0.3\%$) for muons within the angular acceptance that range out.

¹¹For muon identifiers μ_1 , μ_1' , and μ_2 the average ϵ_μ are 0.89, 0.81, and 0.79.

Measurement of Rates for Muonless Deep Inelastic Neutrino and Antineutrino Interactions*

B. Aubert,† A. Benvenuti, D. Cline, W. T. Ford, R. Imlay, T. Y. Ling, A. K. Mann, F. Messing, J. Pilcher,‡ D. D. Reeder, C. Rubbia, R. Stefanski, and L. Sulak
Department of Physics, Harvard University, Cambridge, Massachusetts 02138, and
Department of Physics, University of Pennsylvania, Philadelphia, Pennsylvania 19174, and
Department of Physics, University of Wisconsin, Madison, Wisconsin 53706, and
National Accelerator Laboratory, Batavia, Illinois 60510

(Received 16 May 1974)

Relative rates for deep inelastic neutrino and antineutrino scattering without a final-state muon have been measured. For neutrinos the result is $R^\nu = \sigma(\nu_\mu + \text{nucleon} \rightarrow \nu_\mu + \text{hadrons}) / \sigma(\nu_\mu + \text{nucleon} \rightarrow \mu^- + \text{hadrons}) = 0.11 \pm 0.05$. The corresponding ratio for antineutrinos is $R^{\bar{\nu}} = 0.32 \pm 0.09$.

We have reported previously^{1,2} the observation of deep inelastic neutrino and antineutrino interactions in which no muon appeared in the final

state. In those experiments a value of R , the ratio of the number of events without to the number of events with a muon, was obtained utilizing

mixed neutrino-antineutrino beams with different admixtures. The subject of this paper is the determination of the individual ratios R^ν and $R^{\bar{\nu}}$, appropriate to incident beams of pure neutrinos and pure antineutrinos, respectively.

The experiments were carried out at the National Accelerator Laboratory, where collisions of 300-GeV protons with a target produced secondary hadrons which decay to provide the various neutrino-antineutrino beams. Data for the present study consist of three samples of neutrino- and antineutrino-induced inelastic interactions obtained with the detector, and analyzed by the methods, described in Ref. 2. Each sample is characterized by a different value of α , where α measures the admixture of interacting neutrinos and antineutrinos observed in those events with a muon in the final state; α is the measured ratio of events with negative muons to all events with muons, corrected for the different experimental detection efficiencies for negative and positive muons. Each sample was analyzed to extract the value of R , which is related to R^ν and $R^{\bar{\nu}}$ by

$$R = \alpha R^\nu + (1 - \alpha) R^{\bar{\nu}}. \quad (1)$$

For a pure neutrino or antineutrino beam, Eq. (1) reduces to $R = R^\nu$ or $R = R^{\bar{\nu}}$, respectively.

One of the data samples is essentially the same as that described earlier.² It was obtained with a mixed neutrino-antineutrino beam which was made by focusing negative pions and kaons with a magnetic horn to enrich the antineutrino component. Because the magnetic field of the horn was pulsed on for a period shorter than the duration of the beam spill and a little out of phase with it, the degree of focusing, and hence the mixing parameter, varied with time during each accelerator pulse. The beam spill as a function of time is shown in Fig. 1(a). The variation of α with time is shown in Fig. 1(b). Dividing the da-

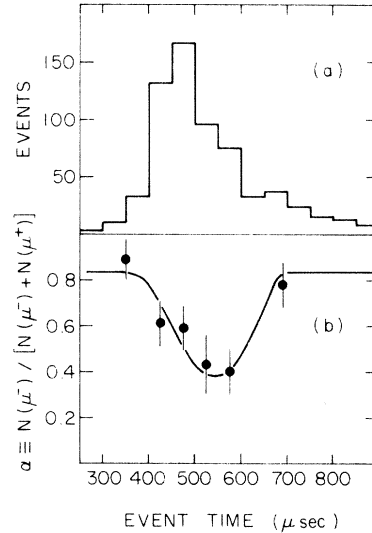


FIG. 1. (a) Distribution of event occurrence times with respect to the start of the master gate. (b) Variation of the neutrino-antineutrino admixture α with event occurrence time, which reflects the on-time of the magnetic horn.

ta into two subsamples, one with a large average value of α and one with a small average value of α , we obtain two relations of the form of Eq. (1) which can be solved for R^ν and $R^{\bar{\nu}}$.

The other two data samples were acquired using essentially pure beams of neutrinos and antineutrinos ($\alpha \approx 0.98$ or $\alpha \approx 0.12$). These beams were produced by sign selection of the charge of the secondary hadrons.³

The analysis of the resulting four data sets is summarized in Table I. As described in Ref. 2, three identifiers of muons were used to provide different muon detection efficiencies ϵ_μ , and different probabilities ϵ_p for the penetration by hadrons of the hadron absorber of a given muon identifier. The three muon identifiers μ_1 , μ_1' , and μ_2 serve to test the internal consistency of our

TABLE I. Summary of data for the four neutrino beam configurations.

Data sample	Number of events	Muon detection efficiency ^a			α	R
		μ_1	μ_1'	μ_2		
Mixed beam, horn off	255	0.86	0.77	0.74	0.74 ± 0.06	0.18 ± 0.05
Mixed beam, horn on	283	0.89	0.81	0.80	0.45 ± 0.06	0.22 ± 0.05
Sign-selected $(\pi, K)^-$	100	0.93	0.87	0.83	0.12 ± 0.05	0.34 ± 0.12
Sign-selected $(\pi, K)^+$	188	0.93	0.87	0.83	0.98 ± 0.01	0.13 ± 0.06

^aThe three muon identifiers μ_1 , μ_1' , μ_2 are defined in Ref. 2.

treatment of the data. The largest solid angle is achieved with μ_1 , but for μ_1' the measured values of ϵ_p are smaller than for μ_1 , and for μ_2 , which has the smallest solid angle, the value of ϵ_p is zero. Furthermore, the dependence of ϵ_μ on the spatial position of the event vertices and on the energy of the hadron cascades of the ν_μ ($\bar{\nu}_\mu$)-induced events is significantly different for the three muon identifiers. The values of the muon-detection efficiencies given in Table I are based on directly measured muon angular distributions using muon identifier μ_1' for each of the data samples.⁴ Included also in Table I are the numbers of events in each sample, the values of the mixing parameter α , and the corrected ratios R . The mean total energy of the events observed is about 45 GeV for the horn beam and about 53 GeV for the sign-selected beams.

Observe that the two subsets of the mixed-beam data (rows 1 and 2) have appreciably different admixtures of ν and $\bar{\nu}$, as indicated by the different values of α , and that the data for the sign-selected beams (rows 3 and 4), with very small and very large values of α , yield R^ν and $R^{\bar{\nu}}$ almost directly and separately.

The maximum-likelihood fit to the four data sets yields $R^\nu = 0.12_4 \pm 0.04$ and $R^{\bar{\nu}} = 0.32_7 \pm 0.08$, where the errors are statistical only. These values include interactions of a small number of electron neutrinos (ν_e) in the incident beams. Electromagnetic showers arising from events with electrons in the final states produced by ν_e ($\bar{\nu}_e$) interactions are not readily distinguished in our detector from hadronic showers induced by ν_μ ($\bar{\nu}_\mu$). Estimates of the ratio $\sigma(\nu_e + \text{nucleon} \rightarrow e^- + \text{hadrons})/\sigma(\nu_\mu + \text{nucleon} \rightarrow \mu^- + \text{hadrons})$ and of the same ratio for $\bar{\nu}_e$ and $\bar{\nu}_\mu$ are (1.7 and 0.5)% respectively. Subtracting these contributions, and folding in an additional uncertainty (arising primarily from the determination of the muon-detection efficiency) of 0.03 in R^ν and 0.04 in $R^{\bar{\nu}}$, we obtain finally $R^\nu = 0.11 \pm 0.05$ and $R^{\bar{\nu}} = 0.32 \pm 0.09$. These results are plotted in Fig. 2 as are also the separate fits to the data taken with the sign-selected beams and the admixed beam. Results from the CERN-Gargamelle experiment⁵ at much lower energy are also included in Fig. 2.

It is clear from Fig. 2 that $R^{\bar{\nu}}$ is larger than R^ν . This may perhaps reflect the experimentally determined fact that the charged weak current cross section for neutrinos σ_c^ν is about 3 times larger than the corresponding cross section $\sigma_c^{\bar{\nu}}$ for antineutrinos in the energy region of these experiments,^{6,7} presumably due to a parity-noncon-

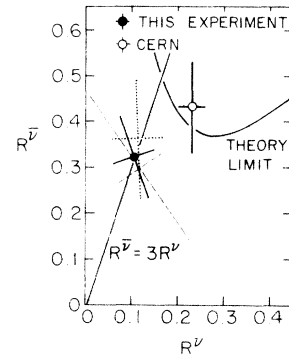


FIG. 2. Results for R^ν and $R^{\bar{\nu}}$ from this experiment. The dotted cross represents results from the sign-selected beams; the dashed cross is from the mixed neutrino-antineutrino beam, for which R^ν and $R^{\bar{\nu}}$ are strongly correlated, as indicated by the orientation of the error bars. The solid circle with its error bars shows the result of a fit to all the data, including systematic errors. All three points are results after subtraction of the ν_e contribution. The open circle point is from Ref. 5. The curve marked THEORY LIMIT is a lower bound obtained from Ref. 11.

serving $V-A$ interference term. If then, for example, the effective neutral weak current cross sections σ_N^ν and $\sigma_N^{\bar{\nu}}$ that give rise to muonless events are equal, one would expect $R^{\bar{\nu}} \approx 3R^\nu$. The locus of the last equation is the line starting at the origin in Fig. 2, which is seen to be consistent with the results of this experiment. Equality of σ_N^ν and $\sigma_N^{\bar{\nu}}$ would imply the absence of a $V-A$ interference term in those cross sections, and, presumably, the absence of parity nonconservation in those processes as well.⁸

In Fig. 2 we show in addition a prediction based on the Weinberg-Salam gauge model⁹ of the weak interactions, in which neutral weak currents make a natural appearance. The extension to semileptonic processes has been made by various authors¹⁰ who obtain the lower bound curve in Fig. 2. Our data are about 2 standard deviations away from that theoretical limit. Within experimental error, other interpretations of the numerical value of $R^{\bar{\nu}}/R^\nu$ are also possible.¹¹ Note that R^ν and $R^{\bar{\nu}}$ may depend on energy, either continuously or discontinuously through some threshold effect, which temporarily, at least, also contributes to the difficulty of delineating the matrix element of the effective neutral weak current.

It is a pleasure to acknowledge the aid and encouragement of the National Accelerator Laboratory staff. We thank D. Cheng and R. L. Piccioni

for their early contributions to this work.

*Work supported in part by the U. S. Atomic Energy Commission.

†On leave of absence from Laboratoire de L'Accelérateur Lineaire, Orsay, France.

‡Alfred P. Sloan Foundation Fellow, now at the University of Chicago, Chicago, Ill. 60637.

¹A. Benvenuti *et al.*, Phys. Rev. Lett. **32**, 800 (1974).

²B. Aubert *et al.*, Phys. Rev. Lett. **32**, 1454 (1974) (this issue).

³See P. Limon *et al.*, NAL Report No. NAL-Pub-73/66-EXP (to be published). During most of the data taking hadrons having a mean energy of 140 GeV were selected, which resulted in a neutrino energy spectrum with a mean energy of 53 GeV and a spread of ± 20 GeV.

⁴To take into account very-large-angle muons it is necessary to make a small correction to the angular distribution data to obtain the detection efficiencies given in Table I. This correction depends on the form of the distribution in the scaling variable $y = E_n/E_\nu$ for events with muons. For antineutrinos the y distribution is not yet definitively determined by our data, but preliminary results suggest that at higher energies the antineutrino distribution is similar to that for neutrinos. Accordingly, we have used the same correction for neutrinos and antineutrinos in conjunction with the measured angular distributions to find the detection efficiencies in the last two rows of Table I. The effect is less than the error assigned to the detection effi-

ciencies in computing the final values of R^ν and $R^{\bar{\nu}}$ and their errors.

⁵F. J. Hasert *et al.*, Phys. Lett. **46B**, 138 (1973), and CERN Report No. TC-L/Int. 74-1 (to be published).

⁶D. H. Perkins, in *Proceedings of the Sixteenth International Conference on High Energy Physics, The University of Chicago and National Accelerator Laboratory, 1972*, edited by J. D. Jackson and A. Roberts (National Accelerator Laboratory, Batavia, Ill., 1973), Vol. 4, p. 189; T. Eichten *et al.*, Phys. Lett. **B46**, 274, 281 (1973).

⁷A. Benvenuti *et al.*, Phys. Rev. Lett. **30**, 1084 (1973), and **32**, 125 (1974).

⁸Suggestions to this effect have been made, for example, by M. A. B. Bég and A. Zee, Phys. Rev. Lett. **30**, 675 (1973); J. J. Sakurai, Phys. Rev. D **9**, 250 (1974); H. Cheng and C. Y. Lo, Massachusetts Institute of Technology Report (to be published).

⁹S. Weinberg, Phys. Rev. Lett. **19**, 1264 (1967). A. Salam, in *Elementary Particle Theory*, edited by N. Svartholm (Almqvist and Forlag, Stockholm, 1968).

¹⁰A. Pais and S. B. Treiman, Phys. Rev. D **6**, 2700 (1972); E. A. Paschos and L. Wolfenstein, Phys. Rev. D **7**, 91 (1973); L. M. Sehgal, Nucl. Phys. **B65**, 141 (1973); C. H. Albright, Phys. Rev. D **8**, 3162 (1973).

¹¹For reviews and extensive references, see E. S. Abers and B. W. Lee, Phys. Rep. **9C**, No. 1 (1973), and M. A. B. Bég and A. Sirlin, to be published. Also A. Pais and S. B. Treiman, U. S. Atomic Energy Commission Report No. COO-2232B-33, 1973 (to be published).

Direct Electron Pair Production by High-Energy Muons

P. L. Jain, M. Kazuno, and B. Girard

High Energy Experimental Laboratory, Department of Physics, State University of New York at Buffalo, Buffalo, New York 14214

(Received 7 December 1973; revised manuscript received 15 April 1974)

By following 280.11 m of track length of 15.8-GeV/ c negative muons in nuclear emulsion, twenty direct electron pairs were observed. For these pairs we have analyzed (i) the total energy distribution, (ii) the energy partition between the two members, (iii) the angular divergence, (iv) the transverse momentum distribution, and (v) the invariant mass of the electron pairs. The experimental results are compared with the present theories.

Many experiments have been performed for the measurements of the direct pair-production cross section with electron primaries,¹ the so-called trident process, but relatively little data are available for the electron pair production through the muon primary.² Among these, a few experimental results agree^{2,3} and others disagree⁴ with theories^{3,5,6} for the observed value of the direct pair-production cross section. Most of the experiments producing electron pairs by either pri-

mary electron¹ or muon² have been performed using cosmic-ray particles. These inherit a common set of difficulties; for example, (i) the pion background is uncertain, (ii) the muons in a particular experiment are not monoenergetic, and (iii) the use of thick targets necessitates serious corrections for multiple scattering and radiation processes. Experiments with primary muons have several advantages over those with electrons. For electron primaries, bremsstrahlung